Discriminating Between Coherent and Incoherent Light with Planar Metamaterials

*T. Frank,[1,2] O. Buchnev,[2,3] T. Cookson,[1] M. Kaczmarek,[1] P. Lagoudakis[1] and V. A. Fedotov[2,3]**
[1] Physics and Astronomy, University of Southampton, SO17 1BJ, UK
[2] Optoelectronics Research Centre, University of Southampton, SO17 1BJ, UK
[3] EPSRC Centre for Photonic Metamaterials, University of Southampton, SO17 1BJ, UK
**email: vaf@orc.soton.ac.uk*

Abstract: Planar metamaterials represent a powerful paradigm of optical engineering, which enables one to control the flow of light across structured material interfaces in the absence of high-order diffraction modes. We report on a discovery that planar metamaterials of a certain type formed by nanopatterned metal films respond differently to spatially coherent and incoherent light, enabling robust speckle-free discrimination between different degrees of light coherence. The effect has no direct analogue in natural optical materials and may find applications in nanoscale metadevices enhancing imaging, vision, detection, communication and metrology.

Keywords: metasurfaces, metamaterials, optical nonlocality, spatial coherence, plasmons

Over the last decade the concept of artificially engineered media (known as metamaterials) has revolutionized the field of optics, pushed the boundaries of microfabrication and stimulated the development of novel characterization techniques.[1,2] Recent demonstrations of anomalous reflection and refraction of light by metasurfaces opened another exciting chapter in optical engineering.[3] Metasurfaces correspond to a class of low-dimensional (i.e., planar) metamaterials and are typically formed by optically thin metal films periodically patterned on the nanoscale. Despite their vanishing thickness, planar metamaterials interact strongly with light, which they can transmit, absorb or reflect in the absence of high-order diffraction modes, effectively acting as optical media of zero dimension in the direction of light propagation. That sets planar metamaterials aside from resonant gratings of various kinds, photonic crystal slabs,[4,5] and perforated metal films exhibiting extraordinary optical transmission.[6] Metasurfaces offer unmatched flexibility in the design and control of light propagation, replacing conventional bulk optical components[7-12] and exhibiting exotic electromagnetic phenomena,[3,13-15] and are fully compatible with existing fabrication processes adopted by CMOS technology.

In this Letter we describe and investigate an intriguing optical phenomenon, whereby the resonant transmission spectra of apparently trivial, metallic planar metamaterials illuminated with spatially coherent and incoherent light do not match even at the qualitative level due to the appearance of new spectral components. The underlying strongly non-local response of the metasurfaces involves neither diffractive coupling to waveguide modes nor lattice resonances, which renders the reported effect as non-trivial. Previously unseen in metamaterials the effect appears to be robust and exceptionally strong, and hence is immediately suitable for practical applications, such as optical metrology, imaging, vision and communication.

The phenomenon was discovered experimentally with nanostructured homogeneous zigzag metasurfaces operating in the near-IR part of the spectrum. The metasurfaces were milled with a focussed ion beam in an 80 nm thick film of amorphous gold sputtered on a 0.5 mm thick fused-quartz substrate. The samples featured complementary versions of the zigzag pattern (Figs. 1a and 1b), which correspond to arrays of continuous nanowires (ZZnW) and their inversion, continuous nanoslits (ZZnS). The nanowires and nanoslits had the width of correspondingly 110 nm and 140 nm. The unit cell of the zigzag pattern contained two straight segments of the nanowire/ nanoslit forming a right angle and had the dimensions of 660 x 520 nm^2, which rendered the zigzag metasurfaces immune to scattering into high-order diffraction modes in the near-IR. The fabricated samples had the area of 21.1 x 20.8 μm^2 and encompassed a total of 1280 unit cells (see Supporting Information).

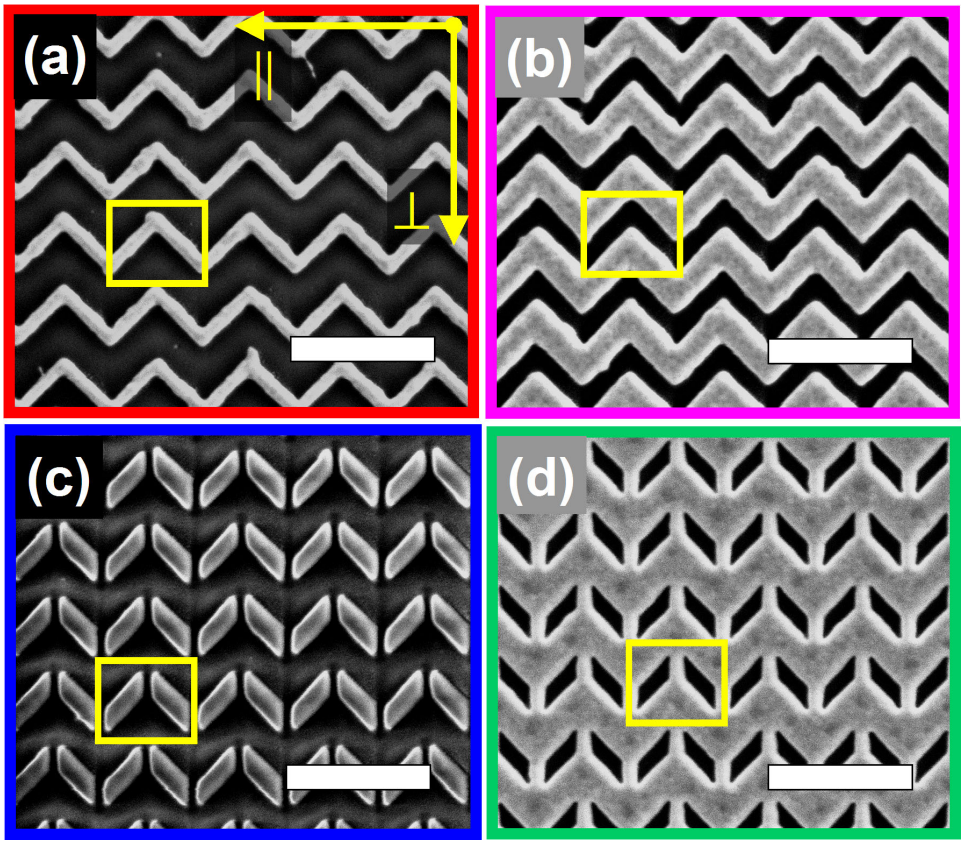

Figure 1. SEM images of fabricated planar metamaterials featuring (a) continuous zigzag nanowires, (b) continuous zigzag nanoslits, (c) broken zizag nanowires, and (d) broken zigzag nanoslits. Yellow boxes indicate elementary unit cells of the metamaterials. Scale bar is 1 μm.

Optical properties of those planar metamaterials were characterized in transmission at normal incidence using a near-IR microspectrophotometer equipped with an incandescent white-light source (WLS) and a broadband linear polarizer. For a ZZnW metasurface, the incident polarization was set perpendicular (⊥) to the rows of the zigzag pattern, while for a ZZnS metasurface the polarization was set in the direction parallel (||) to the zigzag rows, as marked in Fig. 1a. The measured spectra are shown by solid curves in Figs. 2a and 2b. In the wavelength range 0.9 - 1.5 μm both spectra featured a resonance with, what appeared to be, a 0.2 μm wide split. Given the complementarity of the two metamaterials, the profiles of the respective split resonances were also complimentary (as dictated by Babinet's principle): peeks in one spectrum corresponded to dips in the other, and vice versa. Intriguingly, the results of our measurements disagree – even at the *qualitative* level – with the predictions of rigorous numerical modelling that informed the design of our metamaterials (dotted curves in Figs. 2a and b). Indeed, the modelled response in each case displayed a whole resonance centred at $\lambda = 1.1$ μm.[16] It resulted from the excitation of the fundamental $\lambda/2$-current mode – the most common *localized* (dipolar) resonant mode that had been particularly favoured by microwave and RF antennas and planar metamaterials of various designs.[17,18] In the zigzag metasurfaces the mode corresponded to a standing wave of charge oscillations, which built up *locally* in every straight segment of the zigzag pattern, once the half of the wave's period fitted the length of the segment (see insets to Figs. 2a and 2b). That rendered each segment as an independent half-wavelength resonator, which determined the response of the planar metamaterials. The noted strong (and rather unexpected) discrepancy called for careful examination and verification of the methodology used.

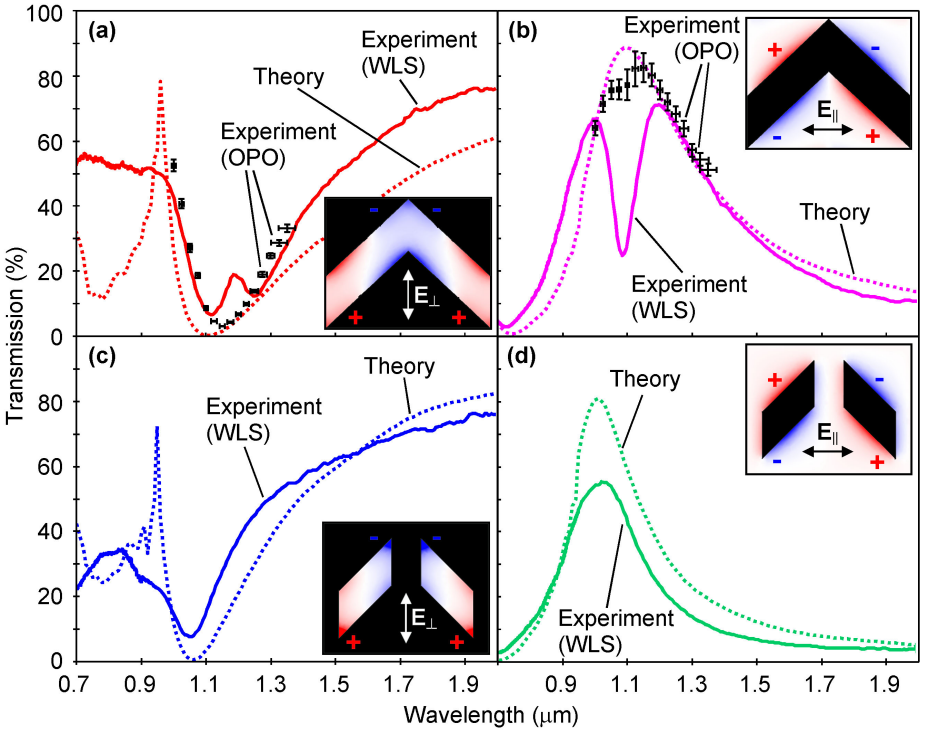

Figure 2. Transmission spectra of zigzag metasurfaces featuring (a) continuous zigzag nanowires, (b) continuous zigzag nanoslits, (c) broken zizag nanowires, and (d) broken zigzag nanoslits. Dashed curves show numerically modelled spectra, which informed the designs of the metamaterials. Solid curves show data measured experimentally using linearly polarized light from incandescent white light source (WLS). Crosses represent data acquired experimentally using linearly polarized light from optical parametric oscillator (OPO). Insets show modelled distributions of charge density induced in the metamaterials' unit cells at resonance (red-blue colors).

For modelling transmission of the zigzag metasurfaces we used a well-established and computationally efficient approach, whereby the simulation domain ($< 4\lambda^3$) accommodated only one unit cell of the modelled metamaterial. The opposite sides of the cell and the faces of the domain contiguous to them were subjected to boundary conditions, periodic in $\perp$ and $\parallel$ directions. The remaining two faces (normal to the direction of light propagation) were terminated with perfectly matched layers (PMLs), with one of the faces set as the source of an electromagnetic wave. The refractive index of fused quartz was set to 1.45[19] and kept constant across the entire spectral range of interest. The dielectric function of gold was defined by the tabulated data.[20] The modelling was implemented with commercial simulation software COMSOL Multiphysics. Experimentally, optical characterization of the zigzag metasurfaces was carried out using a commercial microspectrophotometer developed by CRAIC Technologies on the basis of a ZEISS Axio microscope. It featured a cooled near-IR CCD array with spectral resolution of 0.8 nm and Köhler illumination system, which incorporated a tungsten-halogen lamp and produced broadband quasi-plane wave illumination at normal incidence. Transmitted light was collected using x15 reflective objective with NA 0.28. The spectra of the metamaterials were acquired through a 22 x 22 μm^2 square aperture installed in the image plane of the microscope.

In all the previous works on nanostructured metamaterials, where incoherent illumination with the above (or similar) methodology and instrumentation had been employed, a good agreement between the theory and experiment was reported (see, for example, [21-37]). However, the metamaterials in those studies had one feature in common – their designs were based on piecewise rather than continuous patterns. Thus, the effect we observed must have been overlooked in the interpretation of past experiments. To verify this conclusion we fabricated and subjected to the same testing procedure as above a set of *reference* samples, which resembled ZZnW and ZZnS metasurfaces with broken (i.e. piecewise) zigzags. Their pattern was derived from the original by introducing a 70 nm wide split in every corner of the zigzags, (see Figs. 1c and 1d). Importantly, since the resonant mode supported by the continuous pattern had its nodes located in the corners of the zigzags, the described modification did not affect the nature of the resonant

response in the resulting nanostructures. This is evident from the insets to Figs. 2c and 2d, which show that the localized distributions of charge density sustained by the reference metamaterials at their resonance were very similar to those calculated for the ZZnW and ZZnS metasurfaces. Also, as in the case of continuous zigzags, the transmission spectra predicted for piecewise zigzags featured a whole resonance spanning from 0.9 to 1.5 μm, though its centre appeared blue-shifted by about 50 nm due to physical shortening of the broken segments (dotted curves in Figs. 2c and 2d). In spite of the apparent similarities between the two cases, we were able to reproduce experimentally the main features of the response predicted numerically for the reference samples (solid curves in Figs. 2c and 2d). Some quantitative mismatch resulted from an uncertainty in specifying the dielectric function of gold and the difficulty of reproducing fine features of piecewise zigzags during the fabrication.[16]

Our analysis, therefore, indicated that the discrepancy between the theory and experiment we observed earlier with the ZZnW and ZZnS metasurfaces corresponded to a genuine effect, previously unseen in metamaterials and somewhat exclusive to the continuous pattern. This discrepancy could only have resulted from the difference between the simulated and actual illumination conditions, which thus far had been routinely disregarded in the study of metamaterials: the common modelling approach assumed the complete coherence of incident light, while the spectroscopic measurements involved spatially incoherent light. To verify our conclusion we re-measured the transmission spectra of the ZZnW and ZZnS metasurfaces using a combination of a wavelength-tuneable laser and broadband power meter. The laser source was a quasi-CW optical parametric oscillator (Chameleon Compact OPO) by Coherent with the tuning range 1.00 - 1.35 μm. Linearly polarized OPO output was focussed on the samples to a 50 μm large spot by an achromatic 100 mm lens. Another 100 mm lens was used to collect the transmitted light and direct it towards the power meter. The spectra, which were acquired with the step of 25 nm, are plotted in Figs. 2a and 2b as crosses. Clearly, the new data satisfactory reproduced the predicted resonances. Those measurements thus confirmed that ZZnW and ZZnS metasurfaces could 'sense' the degree of light coherence exhibiting new spectral features under incandescent illumination, which in our case resulted in 3-fold transmission enhancement/ suppression at the resonance wavelength.

The appearance of new spectral features under incoherent white-light illumination had been previously reported for metallodielectric photonic crystal slabs (see, for example,[38]). However, that effect was underpinned by diffractive coupling to *spatially dispersive* waveguide modes (supported by the slabs), which are conceptually not possible in planar metamaterials. Besides, in our case the spilt of the resonance bands was located well away from the wavelength range, where its appearance could have been attributed to the existence high-order diffraction modes or excitation of lattice resonances. Indeed, the excitation of lattice resonances would occur only in the vicinity of the diffraction edge and be most pronounced when the diffraction edge was located on the long-wavelength tail of the unit cell's fundamental resonance.[39] The diffraction edge signifies the appearance of the first diffraction order, which is seen to propagate at a grazing angle. In our case, that would happen in the substrate at the wavelength of ~ 0.96 μm, i.e. well before the metamaterial resonances. Moreover, the appearance of lattice resonances would require the illumination to be of high spatial coherence to ensure proper interference of light scattered by different (distant) unit cells in the array. In practice, this requirement can be met only when focussing optics has a very small numerical aperture (NA < 0.1).[40] Finally, and more crucially, although the zigzag metasurfaces and their reference counterparts had the same period (and the resonant excitations of their individual unit cells had similar nature and strength), the new spectral features were exclusive to continuous zigzag pattern and therefore could not be explained simply by diffractive coupling to lattice resonances.

To understand the nature of the discovered phenomenon we built a comprehensive computational COMSOL model that would enable us to simulate the response of the zigzag metasurfaces to incoherent light. The model featured a large simulation domain (> $46\lambda^3$), where we could faithfully reproduce the entire layout of the samples and, hence, avoid the use of periodic boundaries. Due to memory constrains of our computational hardware, the area of the modelled metamaterial was limited to 10 x 12 unit cells (see Fig. 3a). Also, instead of PMLs, we used scattering boundaries all around – a robust alternative for large simulation domains, which helped us to ease the memory constraints and avoid the difficulty of formulating PMLs near the interfaces.[41] One of the domain's faces parallel to the plane of the metamaterial contained nine

square patches, each set to independently generate a light beamlet with the cross-section of 2.4 x 2.4 μm^2 (purple squares in Fig. 3a). The dimensions of the cross-section matched the spatial coherence length of incandescent light (d_{coh}) at λ = 1.1 μm, estimated according to the expression $d_{coh} = 3.832\ \lambda / 2\pi N_a$.[42] The spectral response to spatially incoherent illumination was given by the sum of the transmission spectra from nine separate runs of the model, each engaging only one particular beamlet. Figure 3b displays the resulting spectrum for the case of a ZZnS metasurface. It features a split resonance resembling very closely what was observed in the experiment under incandescent illumination. Some quantitative mismatch between the measured and calculated data is attributed to an uncertainty in specifying the dielectric function of amorphous gold, as well as to the limitations of our model. In particular, the coherence length (defined by the cross-section of the light beamlets) was kept constant across the entire wavelength range, while the area of the modelled nanostructure was smaller than that of the actual sample by a factor of 10. To confirm that the profile of the calculated spectrum was not an artefact of our modelling approach we compared it in Fig. 3b with the spectrum produced by the model under fully coherent illumination (all nine beamlets were engaged concurrently).

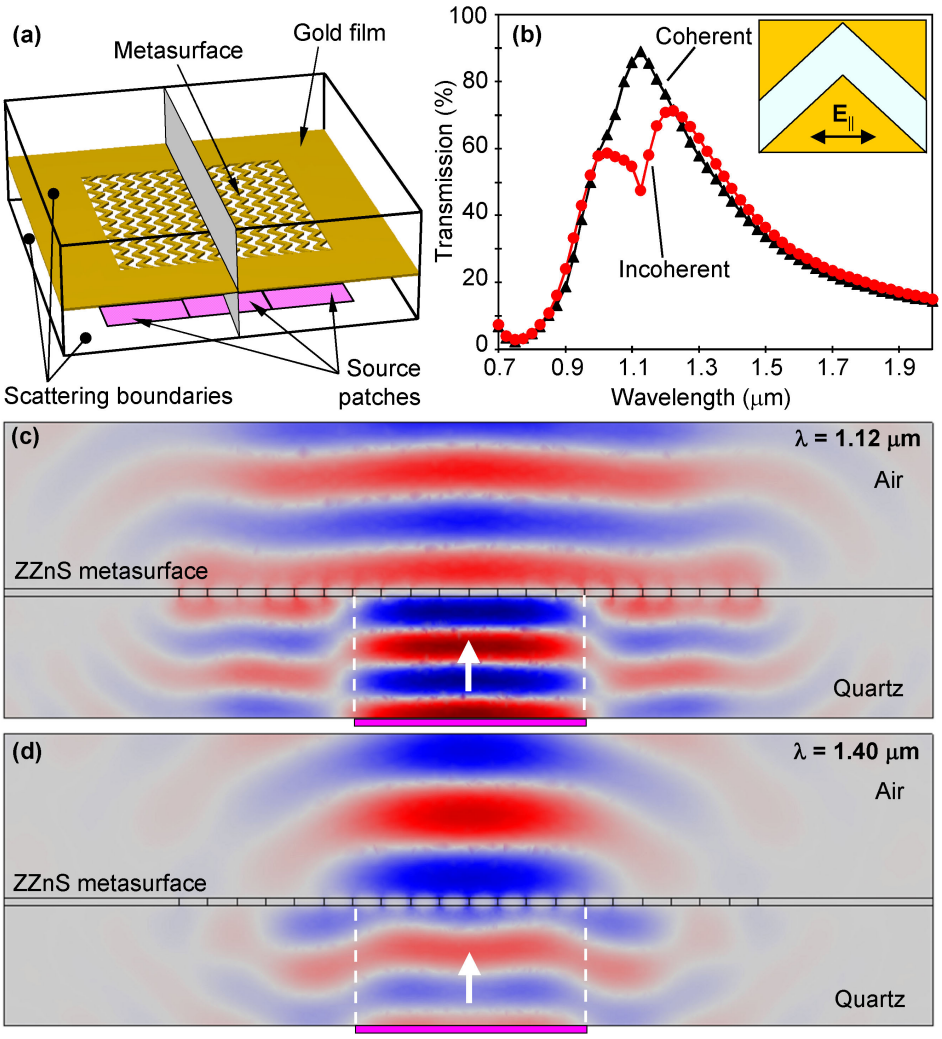

Figure 3. Modelling the response of zigzag metasurfaces to incoherent illumination. (a) Layout of the computational domain. It encompasses a 6.6 x 6.2 μm^2 large metasurface framed by a 2 μm wide strip of unstructured gold film. (b) Modelled transmission spectra of ZZnS metasurface. Data shown by red circles correspond to spatially incoherent illumination. Black triangles show data points calculated for the case of coherent (plane wave) illumination using the same model. (c) Scattering of central beamleat by ZZnS metasurface at the wavelength of 1.12 μm. Color plot maps horizontal component of scattered electric field (its real part) in central cross-section, which splits computational domain in half along zigzag rows, as shown in panel (a). White arrow indicates the direction of incidence, while dashed lines show the extent of incident beamlet. (d) Same as (c) but calculated at the wavelength of 1.40 μm.

The nature of the discovered effect and, more specifically, the origin of the split resonance can be deduced from the distribution of electric field near the ZZnS metasurface calculated at the split's centre wavelength. Such a distribution is plotted in Fig. 3c for the cross-section of the domain that divides the metamaterial in half along the zigzag rows. It pictures a light wave polarized in the plane of the cross-section (||-polarization), which emanates from the central patch at the bottom of the domain and propagates upward as a beamlet until scattered by the nanostructure. While the incident wave is confined laterally to the area of the patch, the transmitted and reflected waves are seen to spread along the plane of the metamaterial far beyond these confines. The resulting field configuration indicates that the mechanism of light scattering by the ZZnS metasurface is extremely non-local. Since planar metamaterials do not diffract as a whole (i.e. do not support high-order diffraction modes) this mechanism must involve plasmon waves, which due to continuity of the pattern can leak from a locally excited unit cell and propagate up and down the zigzags. In the ZZnS metasurface these waves are guided in the form of a mode confined to the nanoslits. It transports the excitation via the zigzag channels to other parts of the metamaterial, where it is radiated and interferes with the fields scattered there locally. Strong local response plays a crucial role here not only by selecting the actual mode that mediates non-local scattering but also by rendering it nondispersive. As we explained earlier, at the resonance of the zigzag metasurfaces the period of the plasmon waves has to fit inside one unit cell exactly.[43] This ensures that only λ/2-mode is sustained by the zigzag channels and all the unit cells engaged in non-local scattering will be driven to the resonance radiating most strongly. More importantly, this guarantees that the radiated fields are all in phase and, hence, add up to form planar wavefronts that stretch wide over the metamaterial, significantly increasing the spatial coherence of scattered light (as evident from Fig. 3c). Nothing of this kind happens outside the resonance (see Fig. 3d).

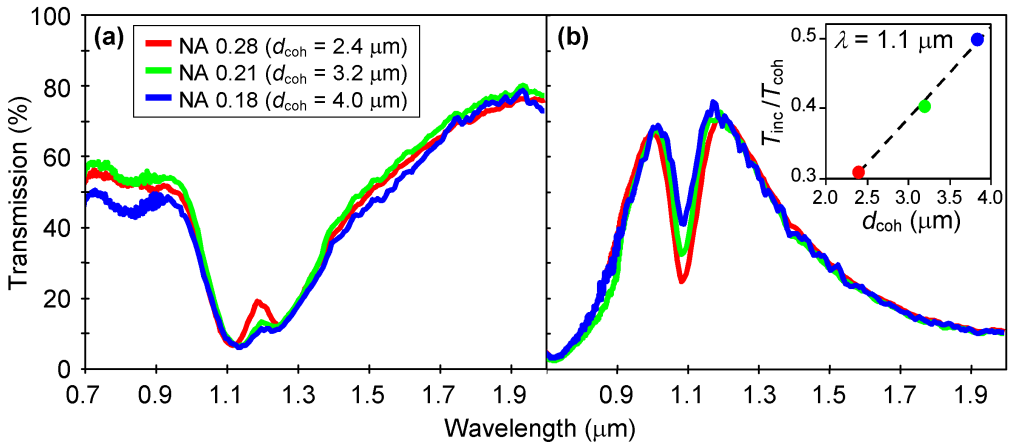

Figure 4. Transmission spectra of (a) ZZnW and (b) ZZnS metasurfaces, which were acquired experimentally for three different values of the coherence length d_{coh}. Inset to panel (b) plots T_{inc}/T_{coh} as a function of d_{coh} calculated for ZZnS metasurface using its transmission data in the main panel (colour circles), and predicted by Eq. (1) based on the value of T_{inc}/T_{coh} at d_{coh} = 2.4 μm (black dashed line).

The total transmitted field then arises as a superposition of the planar wavefronts propagating in the forward direction, which are *sourced* by different unit cells exposed to light. In the case of incoherent illumination the exposed unit cells are excited with random phases and, hence, the planar wavefronts they produce do not interfere, preventing the transmission of a ZZnS metasurface from reaching maximum (see Supporting Information). Under coherent illumination all unit cells oscillate in sync, which ensures constructive interference of the scattered planar wavefronts and, as a result, maximal transmission. The ratio between the levels of transmission for incoherent, T_{inc}, and coherent, T_{coh}, illumination is given by (Supporting Information)

$$\frac{T_{inc}}{T_{coh}} = \frac{d_{coh}}{L\sqrt{2}}, \qquad (1)$$

where L characterizes the extent of non-local scattering, being the maximum distance that an excitation can travel along the zigzags. The upper boundary for L is defined by the plasmon propagation length, which for gold nanostrips does not exceed 10 μm.[44] Correspondingly, for a ZZnS metasurface at λ = 1.1 μm (d_{coh} = 2.4 μm) we obtain a lower estimate for $T_{inc}/T_{coh} \approx 0.2$, which is not too far off the actual ratio of 0.3 measured experimentally.

In the case of a ZZnW metasurface the scattering process at the resonance is very similar to that revealed by Fig. 3c. The only differences are that non-local scattering is mediated by the plasmonic mode of the nanowires, while the field scattered forward propagates alongside the field of the incident wave. Correspondingly, non-local scattering controls reflection of ZZnW metasurface in exactly the same way as it controls transmission of the complimentary ZZnS design (in agreement with Babinet's principle): it reduces the intensity of light reflected by the ZZnW metasurface under incoherent illumination. This translates into an enhancement of transmission, as it was observed in the experiment (Fig. 2a).

Although the discovered effect may appear similar to the resonances of photonic crystal (PhC) slabs and the extraordinary optical transmission (EOT) of perforated metal films (which are well-known manifestations of strongly non-local response), there are three important differences to note. The new effect (i) does not involve surface lattice resonances and diffractive coupling to waveguide modes, (ii) can only be observed in periodic nanostructures composed of locally resonant scatterers (unit cells) and (iii) is underpinned by the excitation of *nondispersive* delocalised plasmon modes. Consequently, while PhC and EOT resonances should thrive on the spatial coherence of incident light (given their purely non-local nature), the new effect emerges only under spatially incoherent illumination. It results in a *qualitative* change of the resonant spectral profile, namely a split, which will gradually diminish with increasing degree of light spatial coherence while remaining pinned to the wavelength of the resonance (the behaviour that is alien to lattice resonances). To confirm this behaviour experimentally we have measured the transmission spectra of the zigzag metasurfaces using the same near-IR microspectrophotometer as before but with a reduced effective numerical aperture (and, hence, increased spatial coherence of illumination). For this study we chose NA 0.21 and NA 0.18, which corresponded to the spatial coherence length of 3.2 μm and 3.8 μm, and were obtained by decreasing the diameter of the condenser's diaphragm by 2 and 4 times, respectively. The measured spectra are plotted in Fig. 4 and compared with the transmission data obtained earlier using NA 0.28 (d_{coh} = 2.4μm). Clearly, the split in the resonances of ZZnW (Fig. 4a) and ZZnS (Fig. 4b) metasurfaces is becoming less pronounced as the coherence length of light increases, but its centre wavelength does not change. Moreover, the inset to Fig. 4b confirms that for the ZZnS metasurface the ratio T_{inc}/T_{coh} scales linearly with d_{coh}, as predicted by Eq. (1).

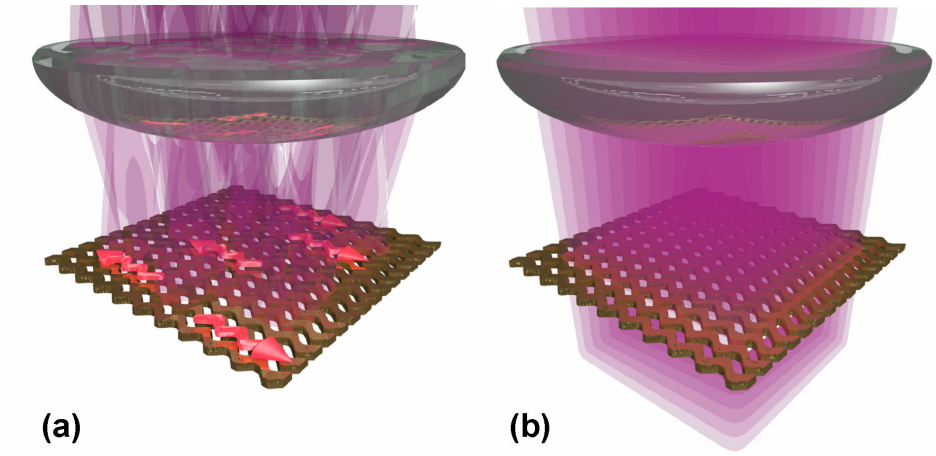

Figure 5. Artistic impression of light transmission by ZZnS metasurface. (a) Spatially incoherent light is rejected through strongly non-local scattering mediated by continuous framework of the metamaterial. (b) Coherent light negates the role of non-local scattering and is fully transmitted.

In summary, we show experimentally and confirm via rigorous numerical modelling that the optical response of metallic planar metamaterials (homogeneous metasurfaces that do not diffract as a whole) may vary dramatically with the spatial coherence of incident light. Illustrated in Fig. 5 this peculiar behaviour previously unseen in metamaterials is characteristic to nanostructured metasurfaces based on a continuous zigzag pattern. Two variants of such metasurfaces imposed by the pattern, namely arrays of zigzag nanowires and zigzag nanoslits, exhibit up to 3-fold decrease/ increase of their resonant transmission depending on the degree of coherence of normally incident light, which is accompanied by a substantial change in the profile of their optical spectra. The mechanism underpinning the new effect involves neither lattice resonances nor diffractive coupling to waveguide modes. Instead, it engages non-local scattering of light via the nondispersive delocalised plasmons supported by *continuous* metallic fabric of the metamaterials. Correspondingly, any continuous periodic metamaterial pattern will exhibit the effect provided that its unit cells locally support the resonant excitation of the symmetric $\lambda/2$-dipole mode. An array of meanders, the so-called fish-scale pattern,[45] is among the potential candidates. The strength and robust nature of the effect make the demonstrated zigzag metasurfaces immediately suitable for optical metrology applications. In particular, combined with a photodetector, a zigzag metasurface represents a very simple and compact optical device that will enable quick quantitative assessment of the spatial coherence of light. Such a device will measure the transmission coefficient of the metasurface at the resonance wavelength under partially coherent illumination which, according to Eq. (1), is a linear function of the coherence length. The rest of the parameters, namely the transmission coefficient under spatially coherent illumination and the extent of the nanostructure's non-local scattering, can be determined only once, during the initial characterisation of the metasurface. The values of the coherence length assessed via such a simple approach will be naturally limited (from above) by the extent of plasmon propagation along the fabric of the metasurface and (from below) by the size of the metamaterial unit cell. Other possible applications will rely on the ability of the zigzag metasurfaces to selectively transmit or block spatially incoherent light, and may include the enhancement of optical imaging, vision, detection and communications.

Acknowledgements. The authors would like to acknowledge the financial support of EPSRC (UK) through grants EP/R024421/1 and EP/M025330/1.

Supporting Information. A large-scale image of the fabricated sample; analytical theory of the discovered effect.

References

(1) Ozbay, E. The magical world of photonic metamaterials. *Opt. Photon. News* **2008,** *19,* 22-26.
(2) Soukoulis, C. M.; Wegener, M. Past achievements and future challenges in the development of three-dimensional photonic metamaterials. *Nat. Photon.* **2011,** *5,* 523-528.
(3) Yu, N.; Capasso, F. Flat optics with designer metasurfaces. *Nat. Mater.* **2014,** *13,* 139–150.
(4) Wang, S. S.; Magnusson, R. Theory and applications of guided-mode resonance filters. *Appl. Opt.* **1993,** *32,* 2606-2613.
(5) Zhou, W.; Zhao, D.; Shuai, Y.-C.; Yang, H.; Chuwongin, S.; Chadha, A.; Seo, J.-H.; Wang, K. X.; Liu, V.; Ma, Z.; Fan, S. Progress in 2D photonic crystal Fano resonance photonics. *Prog. Quantum Electron.* **2014,** *38,* 1-74.
(6) Genet, C.; Ebbesen, T. W. Light in tiny holes. *Nature* **2007,** *445,* 39–46.
(7) Huang, F. M.; Kao, T. S.; Fedotov, V. A.; Chen, Y.; Zheludev, N. I. Nanohole array as a lens. *Nano Lett.* **2008,** *8,* 2469-2472.
(8) Aieta, F.; Genevet, P.; Kats, M. A.; Nanfang, Y.; Blanchard, R.; Gaburro, Z.; Capasso, F. Aberration-Free Ultrathin Flat Lenses and Axicons at Telecom Wavelengths Based on Plasmonic Metasurfaces. *Nano Lett.* **2012,** *12,* 4932-4936.
(9) Ishii, S.; Shalaev, V. M.; Kildishev, A. V. Holey-Metal Lenses: Sieving Single Modes with Proper Phases. *Nano Lett.* **2013,** *13,* 159-163.

(10) Wen, D.; Yue, F.; Kumar, S.; Ma, Y.; Chen, M.; Ren, X.; Kremer, P. E.; Gerardot, B. D.; Taghizadeh, M. R.; Buller, G. S.; Chen, X. Metasurface for characterization of the polarization state of light. *Opt. Express* **2015,** *23,* 10272-10281.
(11) Pors, A.; Nielsen, M. G.; Bozhevolnyi, S. I. Plasmonic metagratings for simultaneous determination of Stokes parameters. *Optica* **2015,** *2,* 716-723.
(12) Pala, R. A.; Butun, S.; Aydin, K.; Atwater, H. A. Omnidirectional and broadband absorption enhancement from trapezoidal Mie resonators in semiconductor metasurfaces. *Sci. Rep.* **2016,** *6,* 31451.
(13) Schwanecke, A. S.; Fedotov, V. A.; Khardikov, V. V.; Prosvirnin, S. L.: Chen, Y.; Zheludev, N. I. Nanostructured metal film with asymmetric optical transmission. *Nano Lett.* **2008,** *8,* 2940-2943.
(14) Menzel, C.; Helgert, C.; Rockstuhl, C.; Kley, E.-B.; Tünnermann, A.; Pertsch, T.; Lederer, F. Asymmetric Transmission of Linearly Polarized Light at Optical Metamaterials. *Phys. Rev. Lett.* **2010,** *104,* 253902.
(15) Plum, E.; Fedotov, V. A.; Zheludev, N. I. Specular optical activity of achiral metasurfaces. *Appl. Phys. Lett.* **2016,** *108,* 141905.
(16) The apparent discrepancy between the calculated and measured spectra in Figs. 2a and 2c below 0.9 μm signifies the appearance of the 1st-order diffraction modes in the substrate due to 660 nm period of the metasurfaces (which acted as conventional diffraction gratings in that wavelength range for light propagating in the substrate). The discrepancy results from the fact that those diffraction modes existed only in the substrate, which for practical reasons was modelled as a semi-infinite slab while in the experiment it had a finite thickness.
(17) Munk, B. A. *Frequency Selective Surfaces: Theory and Design;* Wiley: New York, 2000.
(18) Vardaxoglou, J. C. *Frequency Selective Surfaces: Analysis and Design;* Research Studies Press: Baldock, 1997.
(19) Malitson, I. H. Interspecimen comparison of the refractive index of fused silica. *J. Opt. Soc. Am.* **1965,** *55,* 1205-1208.
(20) Palik, E. D. *Handbook of Optical Constants of Solids;* Academic press: Orlando, Fla., 1985.
(21) Linden, S.; Enkrich, C.; Wegener, M.; Zhou, J.; Koschny, T.; Soukoulis, C. M. Magnetic Response of Metamaterials at 100 Terahertz. *Science* **2004,** *306,* 1351-1353.
(22) Enkrich, C.; Wegener, M.; Linden, S.; Burger, S.; Zschiedrich, L.; Schmidt, F.; Zhou, J. F.; Koschny, Th.; Soukoulis, C. M. Magnetic Metamaterials at Telecommunication and Visible Frequencies. *Phys. Rev. Lett.* **2005,** *95,* 203901.
(23) Liu, N.; Langguth, L.; Weiss, T.; Kästel, J.; Fleischhauer, M.; Pfau, T.; Giessen, H. Plasmonic analogue of electromagnetically induced transparency at the Drude damping limit. *Nature Mater.* **2009,** *8,* 758-762.
(24) Pshenay-Severin, E.; Hübner, U.; Menzel, C.; Helgert, C.; Chipouline, A.; Rockstuhl, C.; Tünnermann, A.; Lederer, F.; Pertsch, T. Double-element metamaterial with negative index at near-infrared wavelengths. *Opt. Lett.* **2009,** *34,* 1678-1680.
(25) Helgert, C.; Menzel, C.; Rockstuhl, C.; Pshenay-Severin, E.; Kley, E.-B.; Chipouline, A.; Tünnermann, A.; Lederer, F.; Pertsch, T. Polarization-independent negative-index metamaterial in the near infrared. *Opt. Lett.* **2009,** *34,* 704-706.
(26) Aydin, K.; Pryce, I. M.; Atwater, H. A. Symmetry breaking and strong coupling in planar optical metamaterials. *Opt. Express* **2010,** *18,* 13407-13417.
(27) Plum, E.; Tanaka, K.; Chen, W. T.; Fedotov, V. A.; Tsai, D. P.; Zheludev, N. I. A combinatorial approach to metamaterials discovery. *J. Opt.* **2011,** *13,* 055102.
(28) Wu, C.; Khanikaev, A. B.; Adato, R.; Arju, N.; Yanik, A. A.; Altug, H.; Shvets, G. Fano-resonant asymmetric metamaterials for ultrasensitive spectroscopy and identification of molecular monolayers. *Nature Mater.* **2012,** *11,* 69-75.
(29) Wu, P. C.; Chen, W. T.; Yang, K.-Y.; Hsiao, C. T.; Sun, G.; Liu, A. Q.; Zheludev, N. I.; Tsai, D. P. Magnetic plasmon induced transparency in three-dimensional metamolecules. *Nanophoton.* **2012,** *1,* 131-138.
(30) Fedotov, V. A.; Uchino, T.; Ou, J. Y. Low-loss plasmonic metamaterial based on epitaxial gold monocrystal film. *Opt. Express* **2012,** *20,* 9545-9550.
(31) Li, Z.; Gokkavas, M.; Ozbay, E. Manipulation of Asymmetric Transmission in Planar Chiral Nanostructures by Anisotropic Loss. *Adv. Opt. Mater.* **2013,** *1,* 482-488.

(32) Benz, A.; Montaño, I.; Klem, J. F.; Brener, I. Tunable metamaterials based on voltage controlled strong coupling. *Appl. Phys. Lett.* **2013,** *103,* 263116.
(33) Fang, X.; Tseng, M. L.; Ou, J. Y.; MacDonald, K. F.; Tsai, D. P.; Zheludev, N. I. Ultrafast all-optical switching via coherent modulation of metamaterial absorption. *Appl. Phys. Lett.* **2014,** *104,* 141102.
(34) Cetin, A. E.; Kaya, S.; Mertiri, A.; Aslan, E.; Erramilli, S.; Altug, H.; Turkmen, M. Dual-band plasmonic resonator based on Jerusalem cross-shaped nanoapertures. *Photon. Nanostruct. Fundament. Appl.* **2015,** *15,* 73-80.
(35) Waters, R. F.; Hobson, P. A.; MacDonald, K. F.; Zheludev, N. I. Optically switchable photonic metasurfaces. *Appl. Phys. Lett.* **2015,** *107,* 081102.
(36) Mbomson, I. G.; Tabor, S.; Lahiri, B.; Sharp, G.; McMeekin, S. G.; De La Rue, R. M.; Johnson, N. P. Asymmetric split H-shape nanoantennas for molecular sensing. *Biomed. Opt. Express* **2017,** *8,* 395-406.
(37) Wang, Q.; Mao, D.; Liu, P.; Koschny, T.; Soukoulis, C. M.; Dong, L. NEMS-Based Infrared Metamaterial via Tuning Nanocantilevers Within Complementary Split Ring Resonators. *IEEE J. Microelectromech. Sys.* **2017,** *26,* 1371-1380.
(38) Linden, S.; Kuhl, J.; Giessen, H. Controlling the Interaction between Light and Gold Nanoparticles: Selective Suppression of Extinction. *Phys. Rev. Lett.* **2001,** *86,* 4688.
(39) Auguié, B.; Barnes, W. Diffractive coupling in gold nanoparticle arrays and the effect of disorder. *Opt. Lett.* **2009,** *34,* 401-403.
(40) Kravets, V. G.; Kabashin, A. V.; Barnes W. L.; Grigorenko, A. N. Plasmonic Surface Lattice Resonances: A Review of Properties and Applications. *Chem. Rev.* **2018,** *118,* 5912−5951.
(41) Oskooi, A. F.; Zhang, L.; Avniel, Y.; Johnson, S. G. The failure of perfectly matched layers, and towards their redemption by adiabatic absorbers. *Opt. Express* **2008,** *16,* 11376-11392.
(42) Fercher, A. F.; Hitzenberger, C. K.; Sticker, M.; Moreno-Barriuso, E.; Leitgeb, R.; Drexler, W.; Sattmann, H. A thermal light source technique for optical coherence tomography. *Opt. Comm.* **2000,** *185,* 57-64.
(43) Since in the near-IR the dispersion of surface plasmons in gold is close to linear, their wavelength can be estimated as $\lambda_g \approx \lambda\,[(1+\varepsilon_s)/2]^{1/2}$, where ε_s is the dielectric constant of the substrate. Correspondingly, at the resonance $\lambda_g/2 = 0.44\ \mu m$ matches almost exactly the length of zigzag segments, 0.45 μm.
(44) Wulf, M.; de Hoogh, A.; Rotenberg, N.; Kuipers, L. Ultrafast Plasmonics on Gold Nanowires: Confinement, Dispersion, and Pulse Propagation. *ACS Photon.* **2014,** *1,* 1173-1180.
(45) Fedotov, V. A.; Mladyonov, P. L.; Prosvirnin, S. L.; Zheludev, N. I. Planar electromagnetic metamaterial with a fish scale structure. *Phys. Rev. E* **2005,** *72,* 056613.